INTERNATIONAL JOURNAL FOR NUMERICAL METHODS IN FLUIDS
Int. J. Numer. Meth. Fluids 2006; **51**:371–383
Published online 20 December 2005 in Wiley InterScience (www.interscience.wiley.com). DOI: 10.1002/fld.1097

A coupled boundary element–finite difference model of surface wave motion over a wall turbulent flow

Mirmosadegh Jamali*,†

Department of Civil Engineering, Sharif University of Technology, Azadi Avenue, P.O. Box 11365-9313, Tehran, Iran

SUMMARY

An effective numerical technique is presented to model turbulent motion of a standing surface wave in a tank. The equations of motion for turbulent boundary layers at the solid surfaces are coupled with the potential flow in the bulk of the fluid, and a mixed BEM–finite difference technique is used to model the wave motion and the corresponding boundary layer flow. A mixing-length theory is used for turbulence modelling. The model results are in good agreement with previous physical and numerical experiments. Although the technique is presented for a standing surface wave, it can be easily applied to other free surface problems. Copyright © 2005 John Wiley & Sons, Ltd.

KEY WORDS: surface wave; turbulence; boundary element method; standing wave; finite difference; boundary layer

1. INTRODUCTION

Detailed knowledge of the flow structure in a wave boundary layer is needed in calculating quantities like wave friction on a floating structure, rate of sediment transport in coastal areas, and energy dissipation in a sloshing tank. In many occasions, the flow is turbulent with the effects confined to the boundary layers at the solid boundaries, and an effective numerical method to couple the flow outside the boundary layer with that inside the boundary layer is desirable. This paper discusses such an effective numerical technique based on a mixed boundary element-finite difference formulation.

The boundary element method (BEM) has been successfully applied to analyse problems in free-surface flows, e.g. see the review by Grilli and Subramanya [1] for nonlinear progressive water wave problems, and the papers by Hamano *et al.* [2] and Heister [3], respectively, for standing waves and two-layer flows. The boundary element approach is attractive for

*Correspondence to: Mirmosadegh Jamali, Department of Civil Engineering, Sharif University of Technology, Azadi Avenue, P.O. Box 11365-9313, Tehran, Iran.
†E-mail: jamali@sharif.edu

Received 24 April 2005
Revised 28 August 2005
Accepted 30 August 2005

free-surface problems because unlike the domain discretization techniques such as finite element and finite difference methods, only the boundary needs to be discretized, leading to considerable savings in computer storage and time.

In application of BEM to linear or nonlinear water waves, the most successful approaches have been based on describing the physical problem by potential flow theory, i.e. neglecting viscous effects on the wave flow. The literature on inclusion of viscous effects in BEM formulation of water waves using potential theory is rare. Grilli *et al.* [4] modelled wave dissipation in a BEM study of wave shoaling on a sandy bed using potential theory by applying a variable synthesized pressure on the free surface. The pressure distribution was chosen in such a way to extract energy from the wave at a given rate. Recently, Jamali [5] presented a numerical technique which extends the capability of BEM in solution of surface water wave problems to laminar boundary layer effects. A BEM formulation of the potential flow in the bulk of fluid was coupled with a finite difference solution of the boundary layer equations to give the complete flow field. The technique was used to determine the damping rate of a standing wave in a tank, and a good agreement with the previous results was obtained.

In this paper, the technique is extended to turbulent boundary layers. A simple mixing length theory is used for turbulence modelling, and the method is applied to turbulent motion of a standing wave in a tank. The objective is to show how the boundary element technique can be effectively used in modelling surface wave motion over a turbulent boundary layer for practical purposes. Compared to a general-purpose CFD package, the technique has the advantage of accuracy and reducing running time and computer storage by avoiding solving equations of motion for the whole domain. The advantage becomes more significant as the fluid domain becomes bigger.

The overview of the paper is as follows. In Section 2, the theory of nonlinear wave motion with a thin turbulent boundary layer is discussed. In Section 3, the mixed BEM–finite difference method is discussed for two-dimensional standing wave motion. Numerical experimentation is carried out in Section 4. The model results are compared with previous physical and numerical experiments in Section 5. This is followed by concluding remarks in Section 6.

2. FORMULATION

Consider the motion of an incompressible, homogenous, viscous fluid in a two-dimensional container as shown in Figure 1. The fluid domain is denoted by Ω, and its boundary by $\Gamma = \Gamma_f + \Gamma_s$, where Γ_f is the free-surface boundary and Γ_s the solid boundaries. The undisturbed depth of the fluid is denoted by h, the container width by W, and the kinematic viscosity of the fluid by v. The coordinate system x–z is located at the lower left corner of the container, and $\mathbf{n} = (n_x, n_z)$ is the unit vector normal to the fluid domain in an outward direction. The free-surface displacement is denoted by η and the velocity vector by $\mathbf{V} = (V_x, V_z)$.

For a viscous motion the velocity vector may be taken as the sum of an irrotational vector $\nabla\phi$ and a solenoidal vector $\mathbf{U}$, i.e. $\mathbf{V} = \nabla\phi + \mathbf{U}$ [6], where ϕ is velocity potential, governed by the Laplace equation

$$\nabla^2\phi = 0 \quad \text{in } \Omega \tag{1}$$

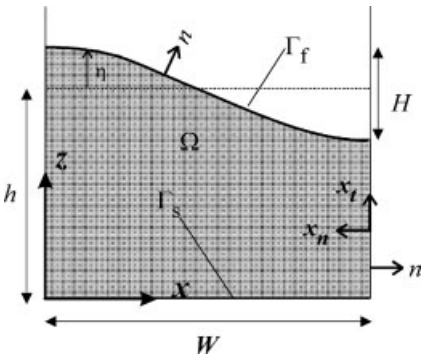

Figure 1. Configuration of the problem.

At high Reynolds numbers, the effect of viscosity may be ignored outside the boundary layers, and the flow can be treated as potential. This implies $|\mathbf{U}| \ll |\nabla\phi|$ outside the boundary layers. Assuming a linear fluid motion inside the boundary layers, the momentum equation is given by

$$\frac{\partial \mathbf{U}}{\partial t} = \nabla.(\nu_e \nabla \mathbf{U}) \quad \text{in } \Omega \tag{2}$$

where ν_e is eddy viscosity. Based on the improved mixing length model of Madsen and Wikramanayake [7], the following equation is assumed for eddy viscosity:

$$\nu_e = \begin{cases} 0.4|u_{*,\max}|x_n & \text{for } x_n \leqslant a_{bl}\delta \\ 0.4|u_{*,\max}|\delta & \text{for } x_n > a_{bl}\delta \end{cases} \tag{3}$$

where $u_{*,\max}$ is the maximum value of the shear velocity $u_* = \sqrt{|\tau_b(t)|\rho}$, $\tau_b(t)$ is instantaneous shear stress at the solid surface, ρ fluid density, δ wave boundary layer thickness, a_{bl} a modelling parameter, and x_n distance from the solid surface. The parameter a_{bl} is the fraction of the boundary layer thickness above the bed over which the eddy viscosity varies linearly. The eddy viscosity is considered constant above the linear portion. This turbulent model was chosen mainly for its simplicity to demonstrate how BEM applications may be extended to turbulence effects. The model is based on physically sound principles and has the advantage of easy implementation for practical purposes [7]. It should be noted, however, that the overall numerical technique is independent of the type of turbulent model used.

The solenoidal velocity component automatically satisfies the equation

$$\nabla \cdot \mathbf{U} = 0 \quad \text{in } \Omega \tag{4}$$

On the free surface Γ_f, i.e. $z = h + \eta(x,t)$, the boundary conditions may be written in a convenient form for BEM implementation as

$$\left(\frac{\partial \phi}{\partial t}\right)_s = -\frac{1}{2}\left(\frac{\partial \phi}{\partial s}\right)^2 + \frac{1}{2}\left(\frac{\partial \phi}{\partial n}\right)^2 + \frac{\partial \phi}{\partial s}\frac{\partial \phi}{\partial n}\tan\beta - g\eta \tag{5}$$

and

$$\frac{\partial \eta}{\partial t} = \frac{1}{\cos \beta} \frac{\partial \phi}{\partial n} \tag{6}$$

[8], where s and n are directed along and outward normal to the free surface, respectively, β is the angle between the free surface and the horizon at the point of interest, and g is gravity acceleration. The operator $(\partial/\partial t)_s$ is the time derivative when a point on the free surface with fixed x is followed. On the solid surfaces Γ_s, the boundary condition is

$$\nabla \phi + \mathbf{U} = 0 \tag{7}$$

Note that outside the boundary layers, the flow motion is considered to be nonlinear, i.e. the nonlinear terms in (5) and (6) are retained, and the free-surface boundary conditions are applied at the unknown level $z = h + \eta(x, t)$. Taking (x_t, x_n) to be the local coordinate system inside the boundary layers as shown in Figure 1, where x_t and x_n are distances along and normal to the solid surfaces, respectively, from (2) and (7), one can write

$$\frac{\partial U_t}{\partial t} = \frac{\partial}{\partial x_n} \left(v_e \frac{\partial U_t}{\partial x_n} \right) \quad \text{in } \Omega \tag{8}$$

$$\frac{\partial \phi}{\partial x_t} + U_t = 0 \quad \text{at } \Gamma_s \tag{9}$$

and

$$\frac{\partial \phi}{\partial x_n} + U_n = 0 \quad \text{at } \Gamma_s \tag{10}$$

where U_t and U_n are the velocity components of $\mathbf{U}$ in directions of x_t and x_n, respectively. Note that inside the boundary layer the flow length-scale normal to the solid surface is much smaller than that along the surface, so in derivation of (8), the derivatives with respect to x_t have been ignored. The shear stress at the solid surface in the local coordinate is approximated by $\tau_b \approx \rho v_e \partial U_t / \partial x_n$.

For turbulence modelling, the boundary Γ_s in (9) is taken to be effectively located at $x_n = x_{n,0}$ where the tangential velocity is assumed to be zero. The parameter $x_{n,0}$ is an empirical constant and depends on the bed roughness K_s. For an artificial bed, it is assumed $x_{n,0} = 0.033 K_s$ [9]. Equations (1), (3)–(6), and (8)–(10) constitute the equations of motion for flow in a container with a turbulent boundary layer.

With the assumption of a thin boundary layer with thickness δ, $\varepsilon = k\delta$ is a small parameter. Considering that δ is the length-scale for variation of the tangential velocity across the boundary layer, it is convenient to define the normalized coordinate

$$\xi = \frac{x_n}{\varepsilon} \tag{11}$$

and re-write Equations (8) and (4) in terms of the new normal coordinate; as a result

$$\frac{\partial U_t}{\partial t} = \frac{\partial}{\partial \xi} \left(\frac{v_e}{\varepsilon^2} \frac{\partial}{\partial \xi} U_t \right) \quad \text{in } \Omega \tag{12}$$

and

$$\frac{\partial U_n}{\partial \xi} + \varepsilon \frac{\partial U_t}{\partial x_t} = 0 \quad \text{in } \Omega \tag{13}$$

Equation (13) can be integrated to yield U_n at Γ_s as

$$U_n|_{\text{solid surface}} = \varepsilon \frac{\partial \left(\int_0^\infty U_t \, \mathrm{d}\xi \right)}{\partial x_t} \tag{14}$$

knowing $U_n \to 0$ at $\xi = \infty$. The computed value for U_n is then used to obtain $\partial\phi/\partial x_n$ at the solid surface using (10). It is seen $\partial\phi/\partial x_n = O(\varepsilon)$ at the solid surface. As the solenoidal velocity vector **U** diminishes outside the boundary layer, Equation (12) is subject to the additional boundary condition

$$U_t = 0 \quad \text{at} \quad \xi = \infty \tag{15}$$

In the following section, Equations (1) and (12) subject to the boundary conditions (5)–(6), (9)–(10), and (14)–(15) are solved numerically using a mixed BEM–finite difference technique. For modelling purposes, the boundary layer thickness δ in (3) is obtained from Fredsoe's equation [10]

$$\delta = 0.15 A_\delta \left(\frac{A_\delta}{K_s} \right)^{-0.25} \tag{16}$$

where $A_\delta = H/(2 \sinh kh)$ is the wave excursion amplitude just outside the boundary layer, and k and H are the wave number and the wave height, respectively.

3. NUMERICAL TECHNIQUE

The aforementioned equations constitute an initial-boundary value problem. The Laplace equation and the boundary layer equation (12) are solved using BEM and a finite-difference technique, respectively. For BEM solution, the fluid boundary Γ is discretized in linear elements by N nodes. At the corners, the 'double nodes' method is used to handle discontinuity of the flux at these points, e.g. see Reference [2]. Many authors have been forced to implement a smoothing procedure to prevent sawtooth instabilities which occur on the free surface after a large number of time steps, see Reference [3]. This is usually done by re-gridding the free surface nodes. However, here the free surface profile is stabilized by adding artificial diffusion terms $\nu_a \partial^2\phi/\partial x^2$ and $\nu_a \partial^2\eta/\partial x^2$ to the right-hand sides of (5) and (6), respectively. A value of $\nu_a = 10^{-6}\,\mathrm{m}^2/\mathrm{s}$ is used in the present calculations. This value was found sufficient to prevent instability while it is still small enough not to affect the flow dynamics.

The boundary layer equations are solved using a Crank–Nicolson scheme. A length of $3/k$ for the domain length in the ξ direction was found sufficiently large to model the infinite boundary $\xi = \infty$. This is equivalent to a distance of 3δ from the solid boundary. With this choice of location of the infinite boundary, the calculations become effectively independent of ε. However, the use of ε reduces computer round-off errors by making the diffusion coefficient in Equation (12) of order unity. The domain was discretized using M equally-spaced grid points with spacing $\Delta\xi$.

The time integration of ϕ, η, and U_t from time t to $t+\Delta t$ is carried out according to the following steps:

Step 1: For the boundary layer above each BEM node on the solid surface, $U_t|^{t+\Delta t}$ is obtained from the finite difference solution of (12) using a Crank–Nicolson finite difference scheme. As the boundary condition at the solid boundary is not known at next time level, it is assumed $U_t|^{t+\Delta t} \approx U_t|^t$ at $\xi = 0$. This introduces an error of $O(\Delta t)$, which can be ignored.

Step 2: $\partial\phi/\partial x_n$ at each BEM node at next time level is calculated from (10) using (14).

Step 3: Equations (5) and (6) with the artificial diffusion terms added are discretized using an explicit scheme to obtain ϕ and η at $t+\Delta t$ on the free surface. Note that $\partial\phi/\partial n|^t$ on the free surface is already available from the solution of Laplace equation at time t.

Step 4: Having η at $t+\Delta t$, the nodes at the free surface are moved to the new location. Then, having ϕ for the free surface nodes and the outward potential flux $\partial\phi/\partial n = -\partial\phi/\partial x_n$ at $t+\Delta t$ from Step 2 for the solid surface, the Laplace equation is solved using the boundary element technique to obtain the potential solution at $t+\Delta t$. For a description of BEM for Laplace equation, the interested reader is referred to numerous textbooks on the subject and the articles by Hamano *et al.* [2] and Grilli and Subramanya [1] on BEM applications to free-surface water waves.

The solution of the Laplace equation gives the potential on the solid surface and $\partial\phi/\partial n$ on the free surface at the time level $t+\Delta t$. From the solution, $U_t|^{t+\Delta t}$ at the solid surface is calculated from (9) using a central difference scheme. For the corner nodes, a one-sided scheme is used.

Starting from $t=0$, Steps 1–4 are repeated at every time step to obtain the solution at the next time level. The initial condition for the potential flow may be obtained from a linear theory, and $\mathbf{U}$ can be considered zero at the start of the simulation.

4. NUMERICAL EXPERIMENTS

Consider a container having the dimensions $W = 2$ m and $h = 0.6$ m in which a first-mode standing wave with height 0.14 m is oscillating in water with $\nu = 10^{-6}\,\mathrm{m^2/s}$. The free-surface boundary and the whole solid boundary are each discretized with 40 nearly equally-spaced nodes for BEM application, and 150 grid points are used for discretization of the boundary layer, so $N = 80$, $M = 150$, and $N_\mathrm{f} = 40$, where N_f denotes the number of BEM nodes on the free surface. The time step $\Delta t = 0.0002$ s was found sufficiently small to give accurate results for the simulation. The boundary layer model parameter $a_\mathrm{bl} = 0.1$, and the sediment bed is assumed to have $K_\mathrm{s} = 0.009$ m. At $t=0$ the standing wave is assumed to have a flat free surface, and the corresponding initial condition is obtained from the linear theory.

Figure 2(a) shows time variation of η at the left and right corners of the free surface. In Figure 2(b) the free surface displacement at instances $t = 4.20\,\mathrm{s} \approx 2.25T$, $t = 4.65\,\mathrm{s} \approx 2.5T$, and $t = 5.12\ \mathrm{s} \approx 2.75T$, where T is the wave period, is presented. It is seen that the free surface has been smoothly simulated with no sawtooth instability. However, a beating effect is observed in the time history of displacement of each corner. This could be because of presence of higher wave harmonics from the nonlinear effects; it is seen in Figure 2(b) that the free surface profile is not completely sinusoidal as the wave node is not located at the

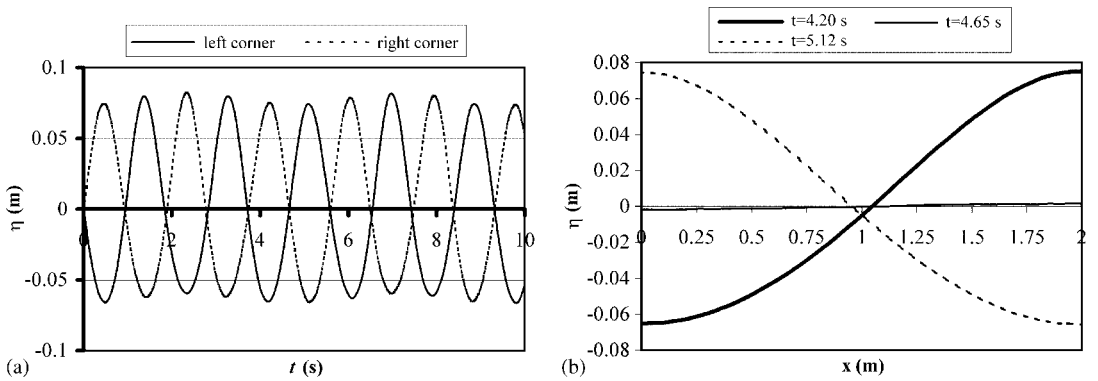

Figure 2. (a) Time variation of the displacements of the left and right corners of the free surface; and (b) profile of the free surface at time intervals of about $T/4$ for $W = 2$ m, $h = 0.6$ m, $H = 0.14$ m, and $v = 10^{-6}$ m^2/s. The discretization parameters are $N = 80$, $N_f = 40$, $M = 150$, $\Delta t = 0.0002$ s, and $a_{bl} = 0.1$.

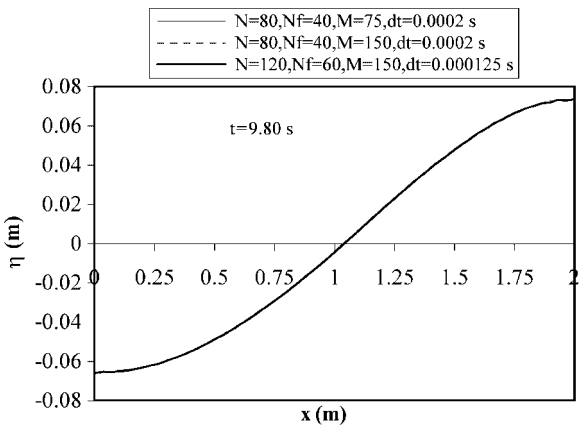

Figure 3. Comparison of profiles of the free surface at $t = 9.80$ s from three different discretizations; $W = 2$ m, $h = 0.6$ m, $H = 0.14$ m, $v = 10^{-6}$ m^2/s, and $a_{bl} = 0.1$.

mid-point of the tank. From the numerical results, $T = 1.867$ s, which is close to the value 1.865 s from the dispersion relation $\omega^2 = gk \tanh(kh)$, where ω is frequency.

To check convergence of the results, simulations were also carried out for a coarse discretization with $N = 80$, $N_f = 40$, $M = 75$ with $\Delta t = 0.0002$ s and a fine discretization with $N = 120$, $N_f = 60$, $M = 150$ with $\Delta t = 0.000125$ s. The results are shown in Figure 3 for the free surface profile at $t = 9.80\,\text{s} \approx 5.25T$ and in Figures 4(a) and (b) for velocity distribution and shear stress distribution, respectively, in the bed boundary layer midway between the walls (under standing wave node) at $t = 9.30\,\text{s} \approx 5T$. The results indicate that the three mesh sizes yield almost the same free surface displacement, and there is little difference between the computed shear stress and velocity distributions from the three mesh sizes. Therefore, convergence is warranted.

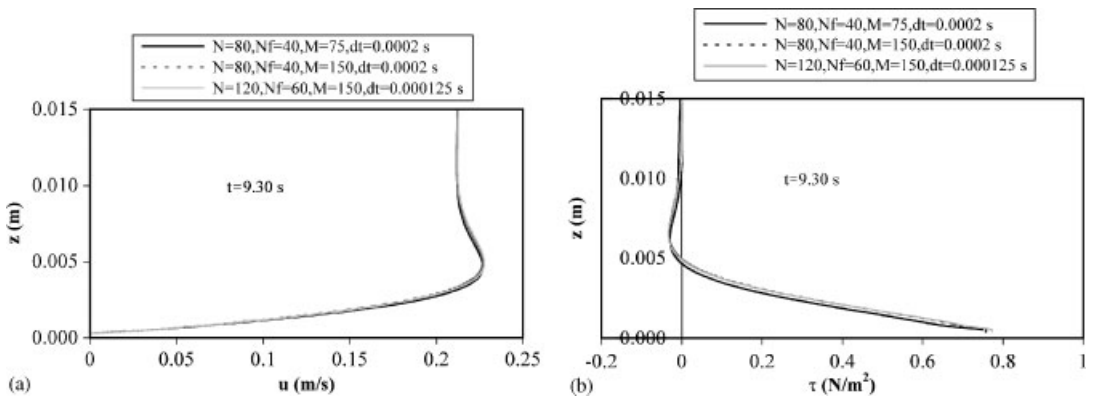

Figure 4. Comparisons of (a) velocity distributions and (b) shear stress distributions in the bed boundary layer midway between the walls at $t = 9.30$ s from three different discretizations; $W = 2$ m, $h = 0.6$ m, $H = 0.14$ m, $v = 10^{-6}\,\mathrm{m^2/s}$, and $a_{\mathrm{bl}} = 0.1$.

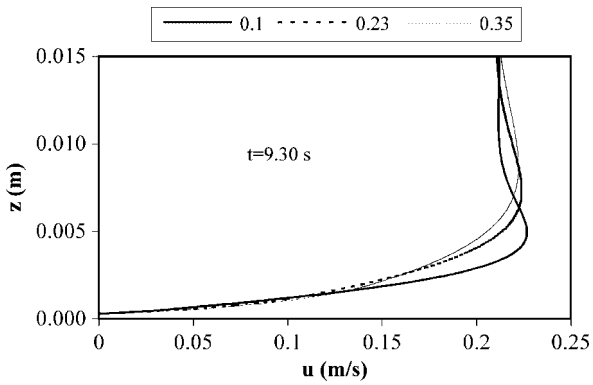

Figure 5. Comparison of velocity distributions in the bed boundary layer midway between the walls at $t = 9.30$ s using $a_{\mathrm{bl}} = 0.10, 0.23$, and 0.35; $W = 2$ m, $h = 0.6$ m, $H = 0.14$ m, and $v = 10^{-6}\,\mathrm{m^2/s}$. The discretization parameters are $N = 80$, $N_{\mathrm{f}} = 40$, $M = 150$, and $\Delta t = 0.0002$ s.

At this point, it is appropriate to do a sensitivity analysis on the boundary layer model parameters a_{bl} and $x_{n,0}$. Figure 5 presents a comparison of velocity distributions in the bed boundary layer midway between the walls at $t = 9.30$ s using $a_{\mathrm{bl}} = 0.1, 0.23$, and 0.35. It is seen that use of a smaller a_{bl} results in a larger overshoot in the velocity profile along with a downward shift in the level of the maximum velocity. This is the same result as obtained by Madsen and Wikramanayake [7]. Figure 6 presents the model results for $x_{n,0} = 0.015K_{\mathrm{s}}$, $0.033K_{\mathrm{s}}$, and $0.066K_{\mathrm{s}}$ with $a_{\mathrm{bl}} = 0.23$. It is seen that a larger $x_{n,0}$ results in a thicker boundary layer and a larger bed shear stress. It should be noted that $x_{n,0} = 0.033K_{\mathrm{s}}$ is usually used for turbulent boundary layer modelling.

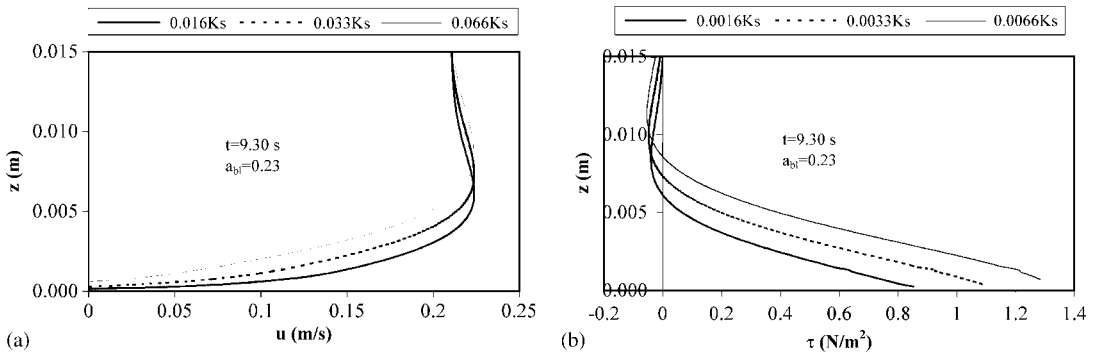

Figure 6. Comparison of profiles of (a) velocity and (b) shear stress in the bed boundary layer midway between the walls at $t = 9.30$ s for $x_{n,0} = 0.015K_s$, $0.033K_s$, and $0.066K_s$; $W = 2$ m, $h = 0.6$ m, $H = 0.14$ m, $\nu = 10^{-6}$ m^2/s, and $a_{bl} = 0.23$. The discretization parameters are $N = 80$, $N_f = 40$, $M = 150$, and $\Delta t = 0.0002$ s.

5. COMPARISON WITH PREVIOUS RESULTS

In this section the model is first compared with the improved model of Madsen and Wikramanayake [7]. Next, the results are compared with the experimental data sets VDW of Van Doorn [11], JC1 and JC2 of Jonsson and Carlsen [12], and numerical experiments DVW05, DVW10, and DVW15 of Davies *et al.* [13]. Davies *et al.* [13] used a different mixing length model. The parameters for these data sets are summarized in Table I.

The conditions of VDW experiment are used to compare the present model and the improved model of Madsen and Wikramanayake [7]. The only difference between the two models is that Madsen and Wikramanayake used $\delta_{bl} = 0.4u^*_{max}/\omega$, while the present model uses Equation (16). For VDW experiment, the present model with $a_{bl} = 0.23$ is equivalent to the improved model of Madsen and Wikramanayake with $a_{bl} = 0.35$. Based on these parameters the results of the two models for the velocity profile in the bed boundary layer for VDW experimental conditions when the free stream velocity is maximum are presented in Figure 7. The discretization $N = 80$, $N_f = 40$, $M = 150$, and $\Delta t = 0.0002$ s was used for the present model. It is seen that the two models yields almost the same result. The small difference between the two can be attributed to numerical factors.

In Figure 8, the model results for $a_{bl} = 0.1$ and 0.23 are compared with the experimental data of Van Doorn [11] for the velocity profile in the bed boundary layer when the free stream velocity is maximum. It is seen that the profile with $a_{bl} = 0.1$ fits the data near the bottom while the profile with $a_{bl} = 0.23$ works better towards the top of the boundary layer.

Figures 9 and 10 present comparisons of the model results for $a_{bl} = 0.1$ and 0.23 with the experimental data JC1 and JC2 of Jonsson and Carlsen [12], respectively, for the velocity profile in the bed boundary layer when the free stream velocity is maximum. The discretization parameters are $N = 80$, $N_f = 40$, $M = 150$, and $\Delta t = 0.001$ s. It is seen that the profiles with $a_{bl} = 0.23$ are in better agreement with the experimental data than the profiles with $a_{bl} = 0.10$ near the bed and towards the top of the boundary layer. However, the level of the overshoot and the magnitude of the overshoot are better represented by the profiles $a_{bl} = 0.10$.

Table I. Parameters for the experimental data sets. $\nu = 10^{-6}\,\mathrm{m}^2/\mathrm{s}$ in all the experiments.

Data set	A_δ (m)	ω (rad/s)	K_s (cm)	$\frac{A_\delta}{K_s}$	$Re = \frac{A_\delta^2 \omega}{\nu}$	Reference
VDW	0.0843	3.142	2.10	4.1	2.2×10^4	Van Doorn [11]
JC1	2.81	0.749	1.59	177.2	5.9×10^6	Jonsson and Carlsen [12]
JC2	1.753	0.873	7.50	23.4	2.7×10^6	Jonsson and Carlsen [12]
DVW05	0.637	0.785	15.0	4.2	3.2×10^5	Davies *et al.* [13]
DVW10	1.274	0.785	15.0	8.5	1.27×10^6	Davies *et al.* [13]
DVW15	1.911	0.785	15.0	12.7	2.86×10^6	Davies *et al.* [13]

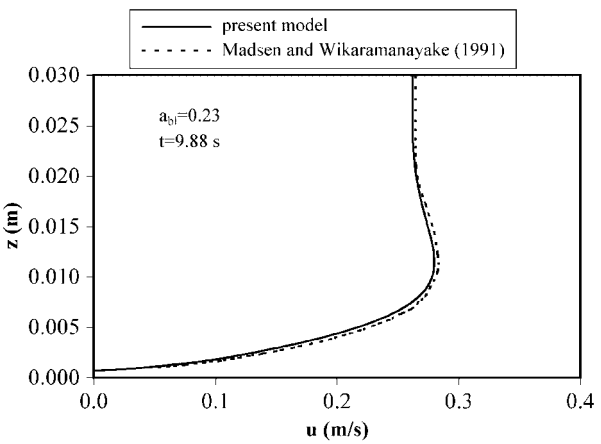

Figure 7. Comparison of the present model and the improved model of Madsen and Wikramanayake [7] for the velocity profile in the bed boundary layer for VDW experimental conditions when the free stream velocity is maximum. The discretization parameters for the present model are $N = 80$, $N_f = 40$, $M = 150$, and $\Delta t = 0.0002\,\mathrm{s}$.

Figure 11 shows a comparison of the instantaneous velocity profiles from the model for $a_{bl} = 0.23$ with the numerical results DVW10 of Davies *et al.* [13] at different phases. The discretization parameters for the present model are $N = 80$, $N_f = 40$, $M = 150$, and $\Delta t = 0.002\,\mathrm{s}$. It is seen that the model results fit well the numerical data close to the bed and towards the top of the boundary layer.

Next attention is paid to the calculated maximum shear stresses in different cases. Based on their improved model, Madsen and Wikramanayake [7] proposed the following expression for the friction factor $f_w = 2\tau_b(t)/\rho u_\infty |u_\infty|$, where u_∞ is the instantaneous free stream velocity just outside the boundary layer, for $(A_\delta/K_s) < 1000$

$$f_w = \exp\left[5.2\left(\frac{A_\delta}{K_s}\right)^{-0.19} - 6.1\right] - 0.24\left(\frac{A_\delta}{K_s}\right)^{-1.2} \tag{17}$$

The maximum shear stresses for the conditions of Van Doorn [11] and Davies *et al.* [13] as calculated by Davies *et al.* [13], the present model with $a_{bl} = 0.10$ and 0.23, and Equation (17)

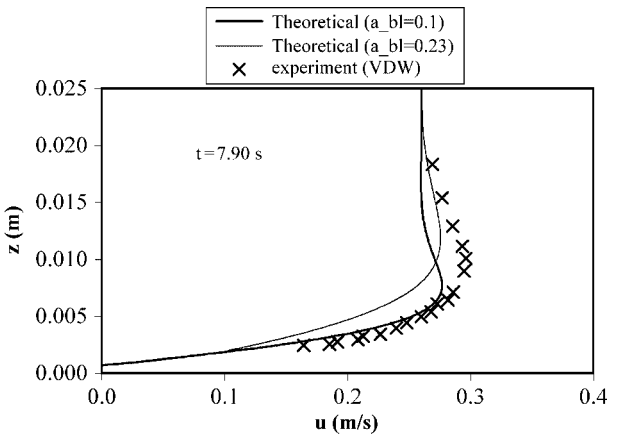

Figure 8. Comparison of the model results for $a_{bl} = 0.10$ and 0.23 with the experimental data VDW (Van Doorn [11]) for the velocity profile in the bed boundary layer when the free stream velocity is maximum. The discretization parameters for the present model are $N = 80$, $N_f = 40$, $M = 150$, and $\Delta t = 0.0002$ s.

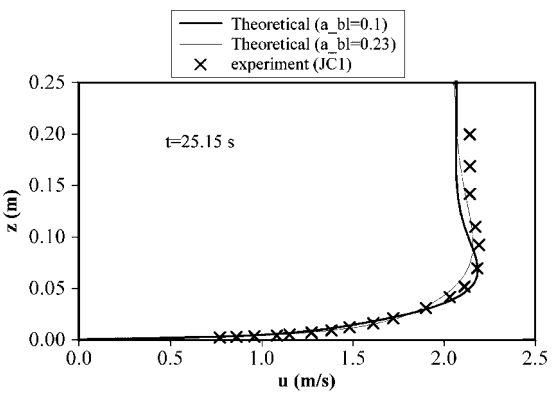

Figure 9. Comparison of the model results for $a_{bl} = 0.10$ and 0.23 for the velocity profile in the bed boundary layer when the free stream velocity is maximum with the experimental data JC1 of Jonsson and Carlsen [12]. The discretization parameters are $N = 80$, $N_f = 40$, $M = 150$, and $\Delta t = 0.001$ s.

are compared in Table II. In general, it is seen that the model results with $a_{bl} = 0.23$ are in better agreement with previous results than are the results with $a_{bl} = 0.10$.

The above comparisons show that the present model has been successful in predicting the boundary layer structure and the bed shear stress. The indications are that for wave conditions a value of $a_{bl} = 0.23$ is the best. The use of a smaller value of a_{bl} usually results in significant changes to the computed velocity and shear stress. These are similar to the results obtained by Madsen and Wikramanayake [7].

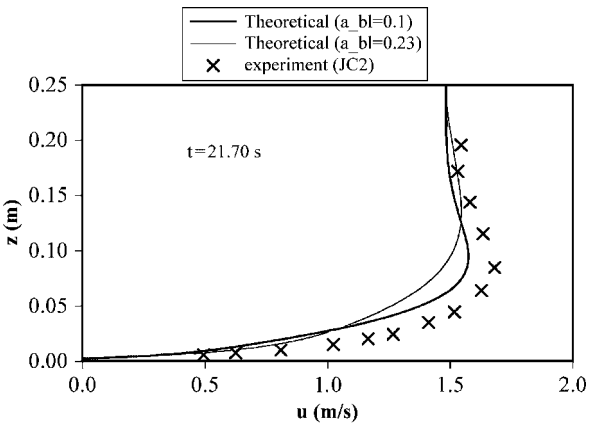

Figure 10. Comparison of the model results for $a_{bl} = 0.10$ and 0.23 for the velocity profile in the bed boundary layer when the free stream velocity is maximum with the experimental data JC2 of Jonsson and Carlsen [12]. The discretization parameters are $N = 80$, $N_f = 40$, $M = 150$, and $\Delta t = 0.001$ s.

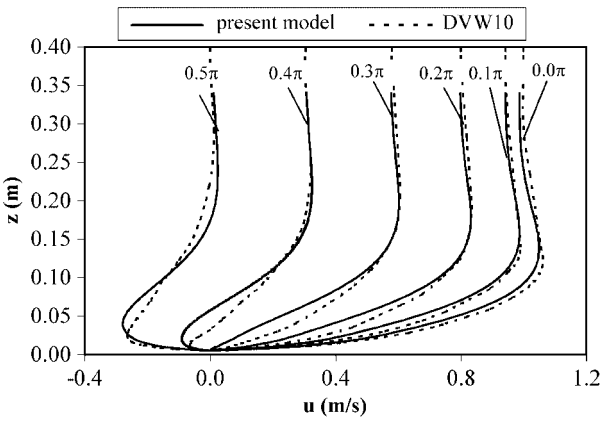

Figure 11. Comparison of the instantaneous velocity profiles from the model for $a_{bl} = 0.23$ with the numerical results DVW10 of Davies *et al.* [13] at different phases. The discretization parameters are $N = 80$, $N_f = 40$, $M = 150$, and $\Delta t = 0.002$ s.

6. CONCLUDING REMARKS

A coupled BEM–finite difference technique was presented to model standing wave motion in a tank with a turbulent boundary layer. The model results are in good agreement with previous experimental and theoretical results.

As the objective of the paper has been to show the possibility of extending BEM capabilities to model turbulence effects, use of a sophisticated turbulent model was avoided for clarity purposes. As such a simple mixing length theory was chosen for turbulent modelling. However, the overall coupling technique is not limited to the turbulent model used, and one may use other models.

Table II. The maximum shear stresses (in N/m^2) for the conditions of Van Doorn [11] and Davies *et al.* [13] as calculated by Davies *et al.* [13], the present model with $a_{bl} = 0.10$ and 0.23, and Equation (17).

			Present model	
Data set	Davies *et al.* [13]	Equation (17)	$a_{bl} = 0.10$	$a_{bl} = 0.23$
VDW	—	2.68	1.53	2.40
DVW05	8.1	9.3	5.8	8.6
DVW10	23.5	26.5	18.5	23.7
DVW15	44.3	49.4	33.0	40.2

In the formulation, the free-surface boundary layer was ignored, and the boundary layer equations for the solid surface were linearized. The proposed technique can be easily extended to include the effect of the free-surface boundary layer and the convection term in the boundary layer equations. The linearized boundary layer equation is appropriate when the surface wave has small amplitude. For large waves, the nonlinear convection term becomes important. This term may be discretized using a simple explicit scheme. Finally, the extension to other free-surface flows including two-layer ones is straightforward.

REFERENCES

1. Grilli ST, Subramanya R. Recent advances in the BEM modeling of nonlinear water waves. In *Boundary Element Applications in Fluid Mechanics*, Power H (ed.). Advances in Fluid Mechanics Series. Computational Mechanics Publication: Southampton, UK, 1995; 91–122 (Chapter 4).
2. Hamano J, Sunao M, Hayami K. Boundary element simulation of large amplitude standing waves in vessels. *Engineering Analysis with Boundary Elements* 2003; **27**:565–574.
3. Heister SD. Boundary element methods for two-fluid free surface flows. *Engineering Analysis with Boundary Elements* 1997; **19**:309–317.
4. Grilli ST, Voropayev S, Testik FY, Fernando HJS. Numerical modeling and experiments of wave shoaling over buried cylinders in sandy bottom. *Proceedings of the 13th Offshore and Polar Engineering Conference* (ISOPE03), Honolulu, USA, May 2003; 405–412.
5. Jamali M. BEM modeling of viscous motion of water waves. *Proceedings of the 23rd International Conference on Offshore Mechanics and Arctic Engineering* (OMAE2004), Vancouver, Canada, June 2004.
6. Morse PM, Feshbach H. *Methods of Theoretical Physics I and II*. McGraw-Hill: New York, 1953.
7. Madsen OS, Wikramanayake PN. Simple models for turbulent boundary layer flow. *Contract Report DRP-91-1*, U.S. Army Corporation of Engineering, Coastal Engineering Research Centre, Vicksburg, Mississippi, 1991.
8. Medina DE, Liggett JA, Birchwood KE, Torrance KE. A consistent boundary-element method for free-surface hydrodynamic calculations. *International Journal for Numerical Methods in Fluids* 1991; **12**:835–857.
9. Van Rijn LC. *Principles of Sediment Transport in Rivers, Estuaries, and Coastal Areas*. Aqua Publications: The Netherlands, 1993.
10. Fredsoe J. Turbulent boundary layer in wave-current motion. *Journal of Hydraulic Engineering* (ASCE) 1984; **110**:1103–1120.
11. Van Doorn Th. Experimental investigation of near-bottom velocities in water waves with and without a current. *Report No. Ml423*, Delft Hydraulics Laboratory, Delft, The Netherlands, 1981.
12. Jonsson IG, Carlsen NA. Experimental and theoretical investigation in an oscillatory turbulent boundary layer. *Journal of Hydraulic Research* 1976; **14**(1):45–60.
13. Davies AG, Soulsby RL, King HL. A numerical model of the combined wave and current bottom boundary layer. *Journal of Geophysical Research* 1988; **93**(Cl):491–508.

